Measured and Modelled Corner Diffraction at Millimetre Wave Frequencies

Thomas H. Barratt[1], Evangelos Mellios[1], Peter Cain[2], Andrew R. Nix[1] & Mark A. Beach[1]
[1]Communication Systems & Networks, University of Bristol
Merchant Venturers' Building, Woodland Road, BS8 1UB, Bristol, United Kingdom
[2]Keysight Technologies, 5 Lochside Avenue, Edinburgh Park, EH12 9DJ, Edinburgh, United Kingdom
Email: [1]{t.h.barratt, evangelos.mellios, andy.nix, m.a.beach}@bristol.ac.uk [2]peter_cain@keysight.com

***Abstract*—Due to spectrum congestion in the commonly used mobile sub-6GHz frequencies, research and measurements in the Millimetre Wave (30-300GHz) bands are required to better understand the medium for 5G and beyond wireless connectivity. In this paper corner diffraction is investigated for an indoor environment in a modern building using a wideband (2GHz) channel sounder at 60GHz. Corner diffraction was measured at five different distances from the corner of interest, with parallel tracks at distances of 0.5m, 1m, 1.5m, 2m and 10m. These measurements were then compared with a Knife Edge Diffraction (KED) model where a 'good-fit' was observed. Results showed that for 2m parallel tracks the power fell by 30dB as the user moved just 0.5m into the shadow region. For a 10m parallel track, the same effect was observed after moving 1.2m into the shadow region. Such rapid changes in received power can adversely affect the performance of link adaptation and beam tracking algorithms as well as the efficiency of the higher layer network protocols.**

Keywords—Millimetre Wave; Knife Edge Diffraction (KED); Corner Diffraction

I. INTRODUCTION

With the advancement of handheld technology, the ever growing demand for wireless connectivity continues at pace. Currently carriers are struggling to meet the service demands of their existing networks despite access to additional frequencies as a result of analogue TV switch off and the release of military bands. In addition, with LTE now having >31 different frequency bands globally, this is causing new issues for 4G network operators due to segmented spectrum. In order to meet the user rates demanded for 5G, new technologies are required. One leading solution for 5G and beyond networks is the use of Millimetre Wave (30-300GHz) spectrum. This is now possible due to advancements in small, low cost and low power CMOS devices [1]. This spectrum can offer large continuous bandwidths that allow multi-gigabit per second data rates [1].

Currently the IEEE 802.11ad standard has created considerable interest in the use of 60GHz unlicensed spectrum [2]. Manufacturers [3] are working on designing and building on-chip transceivers with several devices now commercially available. This marks the beginning of commercial devices that utilise the mmWave bands for wireless communication. Clearly, the 802.11ad standard has created demand for 60GHz on-chip transceivers that offer up to 2GHz of bandwidth and yield theoretical speeds of up to 7Gbps.

In the mmWave bands there is a need to analyse the impact of blocking objects, including the role of diffraction [5-7]. In this paper we use predictions from a mmWave corner diffraction model to compare against measured power levels from a high resolution channel sounder [8, 9].

Indoor corner diffraction is studied by taking measurements every 4mm along five linear tracks. These tracks were placed 0.5m, 1m, 1.5m, 2m and 10m away from the wall edge. Our calibrated wideband measurements were then compared with Knife Edge Diffraction (KED) theory at 60GHz and at 3.5GHz. The rate at which the power falls as the receiver moves into the diffraction shadow region is of particular interest since this can impact the performance of the PHY and MAC layers, as well as the efficiency of the higher layer network protocols.

II. DIFFRACTION

The physical wireless channel is built-up of many different propagation mechanisms including diffraction, reflection, transmission and scattering, all of which connect the transmitter to the receiver through various degrees of dynamic signal attenuation. This paper is focused on a detailed analysis of single corner diffraction in an indoor environment.

Diffraction allows the propagation of radio waves around objects. A commonly used model for this mechanism is Knife Edge Diffraction (KED) [10]. This calculates the attenuation arising from the vector sum of the secondary Huygen's source points in the plane of the knife-edge. This can be calculated using the Fresnel integral [11].

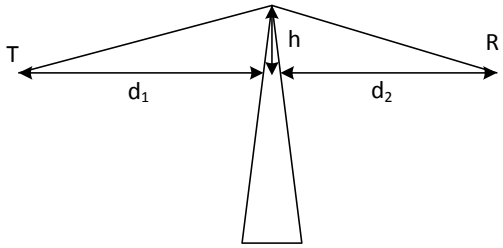

Figure 1: Model for Knife Edge Diffraction (KED) [10]

Knife-edge diffraction theory is predominantly used to model narrow blockages such as roofs as seen in [5, 10, 12], whereas here corner diffraction is considered. The KED model

is illustrated in Figure 1 where T and R represent the transmitter and receiver locations respectively. The model in Figure 1 can be used to calculate the received power of the diffracted signal path using equations (1) and (2) below:

$$v = h\sqrt{\frac{2(d_1+d_2)}{\lambda d_1 d_2}} \quad (1)$$

$$G_d(dB) = 20log|F(v)| \quad (2)$$

where d_1 and d_2 are the distances between the diffracting object and the transmitter or receiver (as shown in Figure 1), h is the height of the object with respect to the direct link between the transmitter and the receiver (also indicated in Figure 1), λ is the wavelength, $G_d(dB)$ is the received gain, and $F(v)$ denotes the Fresnel integral which is geometry-dependent on the Fresnel parameter v [11]. The above equation can therefore be used to calculate the gross signal variation arising from shadowing at the corner and the diffraction process at the edge.

III. Experimental Setup

This section describes the setup of the mmWave diffraction experiments, including an overview of the hardware configuration and a description of the locations of the measurement campaign.

A. Hardware Configuration

A wideband channel sounder was placed on a trolley and pulled along the floor adjacent to the corner under investigation using a series of tracks parallel to the wall, as shown in Figure 2. A 2GHz wide baseband signal was generated using Keysight M9099 Waveform Creator software and used to configure a Keysight M8190A arbitrary waveform generator (ARB). This was then used to drive the I & Q ports on a Sivers IMA up-converter, thus producing a 60GHz modulated carrier [13]. At the receiver a Sivers IMA device down-converts the 60GHz signal to an IQ IF signal and this is then captured and processed using a high performance digital oscilloscope (DSO), MSOS804A.

The Keysight 89600 VSA & Waveform Creator channel sounding function operates by repeatedly transmitting a single carrier signal bearing a modulated waveform. The waveform has excellent auto-correlation properties, and a low peak-to-average power ratio. The bandwidth and duration of the modulating waveform may be varied to suit the channel measurement required. Spectrum shaping can be applied to reduce out of band interference when transmitting the signal in a live environment.

The configuration of the analysis software is set to match the transmit waveform. The measurement receiver hardware needs to capture at least one complete interval of the transmitted waveform, but does not need to be triggered. The measurement is tolerant of small frequency offsets between the transmitter and receiver, meaning the system does not require shared, or particularly demanding frequency references. A proprietary correlation function is applied to the captured data samples using the expected waveform, which results in the recovery of the channel's complex impulse response (and frequency response). This complex channel impulse response (CIR) allows analysis of the phase relationship between paths in the channel. The recovery of the channel coefficients as vector quantities also allows averaging to be used to increase the signal-to-noise ratio (SNR).

The transmitter and receiver employed 20dBi standard gain horn antennas from Flann Microwave, positioned such that all measurements were taken using horizontal polarization. The angular direction of the horns remained constant throughout the experiment and can be seen with the transmitter facing right and the receiver left in the map layout in Figure 2(b).

The channel sounder for these measurements has been configured for external trigger, which is sourced from a shaft encoder mounted on a wheel of the measurement trolley. This creates a trigger every 4mm, with the equipment capable of recording at a sample rate above waking space.

B. Measurment Locations

Our measurements relate to a corner within the Café area of Merchant Venturers' Building (University of Bristol, UK). Diffraction from this corner was measured at multiple distances from the wall as shown in Figure 2. These measurements capture the transition from the Line-of-Sight (LoS) region into the shadow (Non-LoS) region.

The transmitter was positioned 1m from the wall and 5m

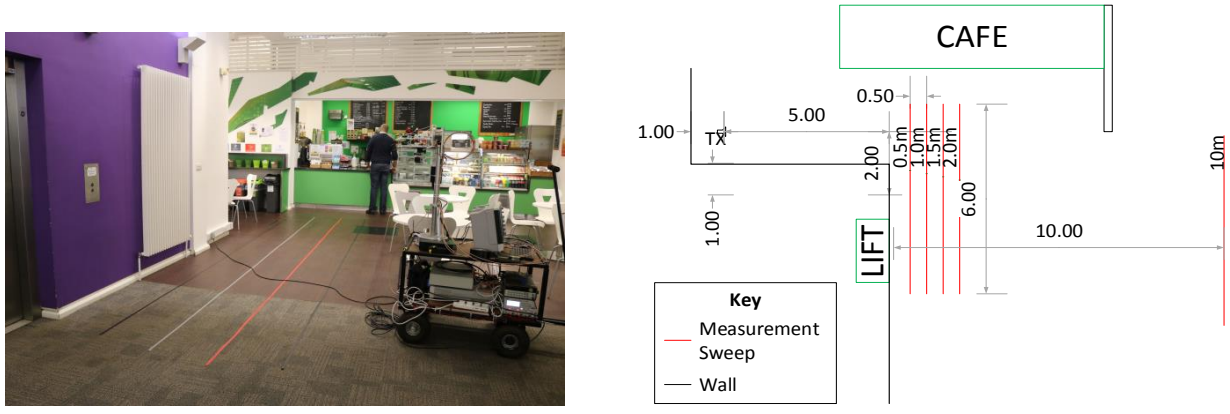

(a) (b)

Figure 2: Photograph (a) and map layout (b) of measurement locations.

from the corner. The receiver was 'pulled' along a 6m route with tracks at 0.5m, 1m, 1.5m, 2m and 10m from the wall. The first 4 tracks started at a distance of 2m from the level of the corner while the 10m run started at a distance of 1m from the level of the corner due to the presence of fixed obstacles. For all cases, a complex CIR was sampled every 4mm. This was repeated 3 times for each run. Figure 3 shows a photograph taken during the measurements and indicates the transmitter position, the receiver on the trolley, and the corner under investigation.

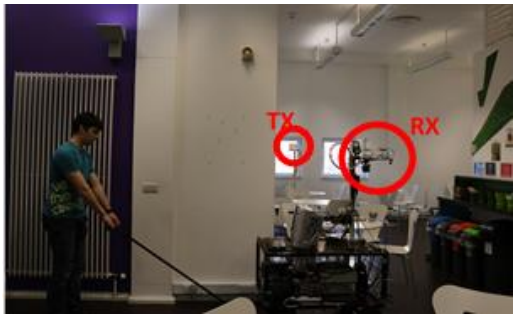

Figure 3: Measurement location, showing transmitter, receiver and corner under investigation.

IV. Results

This section presents the results of the measurement campaign, as well as a comparison with the theoretical KED model at 60GHz as well as 3.5GHz. It should be noted that the impact of the transmit and receive antenna spatial radiation pattern was de-embedded from the measured data in order to obtain the response of the channel (rather than the combined response of the channel and antenna system). Since the antennas' orientation remained stationary during the measurements, this was achieved by normalizing the measured power to an antenna pattern gain measured inside our anechoic chamber.

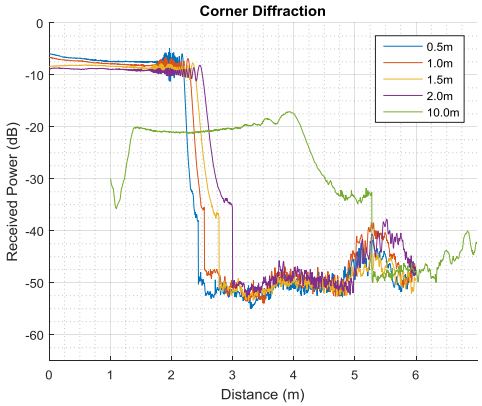

Figure 4: Received power vs Distance for all runs.

Figure 4 shows received power vs distance for each of the five measurement runs. The wideband received power in all cases was normalised relative to that observed at a 1m separation distance. The key observation in Figure 4 is the dramatic drop in received power at the point of corner diffraction (i.e. the diffraction shadow boundary). There are five different distances from the wall and these varied the position along the route where the shadow boundary occurred. Note: due to an unmovable obstacle the 10m run had to start 1m further back. It was observed that a second wall obstructing the start of the 10m run also shows a diffraction effect. Based on our calculations, the LoS path for the 10m run was expected to appear at 1.18m, which can be seen in the graph.

Another key observation is that increasing the distance from the wall also increases the distance from the shadow boundary where the power drops by 30dB. For the 2m run it can be seen it takes 0.5m for a drop of 30dB, whereas for the 10m run a distance of 1.2m is required. Furthermore, an increase in the signal power can be seen between approximately 5m and 6m along the track (for the measurements at a distance of 0.5m to 2m from the corner). This is due to a double reflection path from the metal lift door and another wall directly opposite as shown in Figure 5.

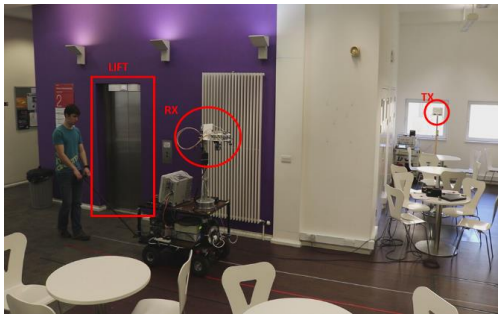

Figure 5: Measurement setup showing lift door.

Using KED theory, a comparison was performed between the theoretic and measured results from the 2m run. The (normalised) results are shown in Figure 6.

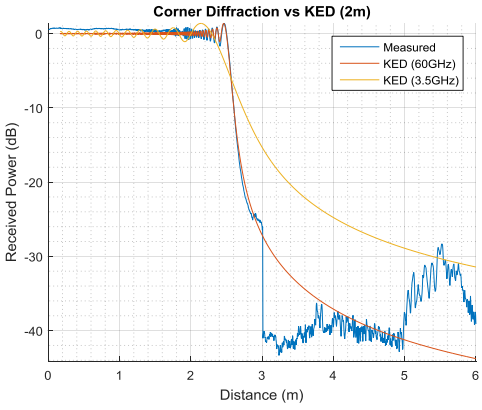

Figure 6: Corner Diffraction 2m: Modelled vs Measured.

Figure 6 demonstrates a very good fit between the measured results and the KED theory. A comparison with a sub-6GHz carrier (3.5GHz) using KED theory is also shown in

Figure 6. An attenuation of 30dB is seen just 30cm into the shadow region at 60GHz, however at 3.5GHz this extends to 2.5m. In the sub-6GHz bands the diffracted power is seen to drop at a lower rate, thus giving the radio and its higher layer protocols more time to adapt. In the mmWave bands the radios will need to adapt at a far faster rate. Figure 6 also shows that the level of diffraction loss is far higher in the mmWave bands. Based on the KED data, the diffraction loss at 60GHz is around 10dB more than that seen at 3.5GHz.

The received power at the diffraction region around the corner point can be seen in more detail in Figure 7, where a comparison between the modelled and measured results is presented. This shows an extremely good fit and highlights constructive and destructive interference of the signal paths in the region just before the transition from LoS to Non-LoS.

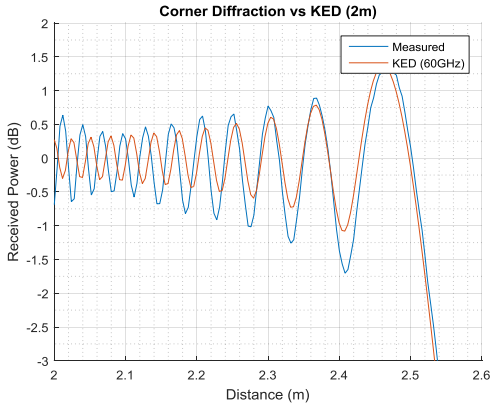

Figure 7: 2m KED vs measured: highlighting constructive and destructive interference.

Finally, Figure 8 shows the calculated KED result compared against the 10m measurement run.

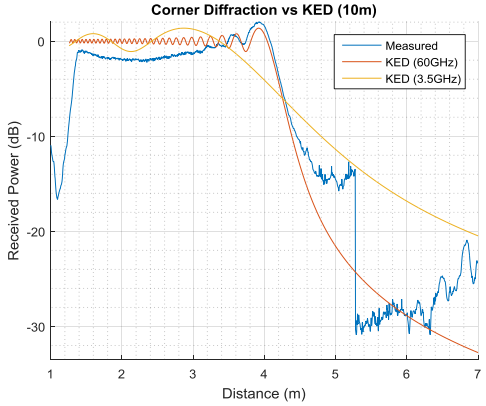

Figure 8: 10m Run - Measured results compared with KED for 60GHz and 3.5GHz.

Again, a good fit is observed in Figure 8 between the measured results and the KED predictions. Figure 8 also presents the predicted received power at 3.5GHz, highlighting once again the smoother transition between LoS and Non-LoS at lower frequencies in comparison to the mmWave bands.

V. Conclusions

This paper has presented results from an isolated corner diffraction measurement campaign in an indoor environment of a modern building. A wideband (2GHz) channel sounder was used at a carrier frequency of 60GHz. The effect of diffraction was measured for five different distances away from the point of interest, with parallel tracks at distances of 0.5m, 1m, 1.5m, 2m and 10m. Measurements were recorded every 4mm over a 6m route.

The data captured from the five measurement runs was seen to align well with KED theory when the spatial characteristics of the directional antennas were de-embedded from the measurement data. The measured results showed that for a parallel track at a distance of 2m from the corner the power fell by 30dB once the user had moved just 0.5m into the shadow region. Using KED theory for a frequency of 3.5GHz, an attenuation of 30dB required movement of 2.5m into the shadow region for the same scenario. For a parallel track at a distance of 10m from the corner of interest, the 60GHz measurements showed that the same effect was observed after moving 1.2m into the NLoS region.

In the sub-6GHz bands the diffracted power was seen to drop at a lower rate, thus giving the radio and its higher layer protocols more time to adapt. In the mmWave bands the radios must adapt at a far faster rate. This may introduce new challenges in the PHY and MAC design as well as the need to re-optimise parameters in the higher layer network protocols.

Finally, we saw that the level of diffraction loss was far higher in the mmWave bands (meaning scattering becomes the dominant multipath effect). Based on our KED analysis the diffraction loss at 60GHz was around 10dB more than that seen at 3.5GHz. It is thus questionable as to whether diffraction needs to be modelled in mmWave ray tracing models.

VI. Acknowledgments

This research was funded as part of the EPSRC Centre for Doctoral Training in Communications (EP/I028153/1) and also the European Commission H2020 programme under grant agreement n°671650 (5G PPP mmMAGIC project).

References

[1] http://www2.imec.be/be_en/research/wireless-communication/60ghz-wireless-communication.html, accessed 31/03/2016.

[2] T. S. Rappaport, S. Shu, R. Mayzus, Z. Hang, Y. Azar, K. Wang, *et al*., "Millimeter Wave Mobile Communications for 5G Cellular: It Will Work!," *Access, IEEE,* vol. 1, pp. 335-349, 2013.

[3] http://www.latticesemi.com/en/Products/mmWave/SiBEAM80211ad Chipsets.aspx, accessed 31/03/2016.

[4] D. E. Berraki, T. H. Barratt, M. A. Beach, S. M. D. Armour, and A. R. Nix, "Practical Demonstration of Limited Feedback Beamforming for mmWave Systems," in *Vehicular Technology Conference (VTC Spring), 2015 IEEE 81st*, 2015, pp. 1-5.

[5] A. K. M. Isa, A. Nix, and G. Hilton, "Impact of diffraction and attenuation for material characterisation in millimetre wave bands," in *Antennas & Propagation Conference (LAPC), 2015 Loughborough*, 2015, pp. 1-4.

[6] Z. Hang, R. Mayzus, S. Shu, M. Samimi, J. K. Schulz, Y. Azar, *et al*., "28 GHz millimeter wave cellular communication measurements for reflection and penetration loss in and around buildings in New York city," in *Communications (ICC), 2013 IEEE International Conference on*, 2013, pp. 5163-5167.

[7] M. Jacob, S. Priebe, R. Dickhoff, T. Kleine-Ostmann, T. Schrader, and T. Kurner, "Diffraction in mm and Sub-mm Wave Indoor Propagation Channels," *IEEE Transactions on Microwave Theory and Techniques*, vol. 60, pp. 833-844, 2012.

[8] R. Luebbers, "Finite conductivity uniform GTD versus knife edge diffraction in prediction of propagation path loss," *IEEE Transactions on Antennas and Propagation*, vol. 32, pp. 70-76, 1984.

[9] N. Tervo, C. F. Dias, V. Hovinen, M. Sonkki, A. Roivainen, J. Meinil, *et al*., "Diffraction measurements around a building corner at 10 GHz," in *5G for Ubiquitous Connectivity (5GU), 2014 1st International Conference on*, 2014, pp. 187-191.

[10] T. S. Rappaport, *Wireless communications : principles and practice*, 2nd ed. Beijing: Publishing House of Electronics Industry, 2012.

[11] R. Vaughan and J. B. Andersen, *Channels, propagation and antennas for mobile communications*. London: Institution of Electrical Engineers, 2003.

[12] J. S. Lu, P. Cabrol, D. Steinbach, and R. V. Pragada, "Measurement and Characterization of Various Outdoor 60 GHz Diffracted and Scattered Paths," in *Military Communications Conference, MILCOM 2013 - 2013 IEEE*, 2013, pp. 1238-1243.

[13] SiversIMA. (2016, Mar 17). *SiversIMA Converters and Customized Transceivers*. Available: http://siversima.com/products/converters-customized-transceivers/